https://doi.org/10.3311/PPee.19858

Periodica Polytechnica Electrical Engineering and Computer Science, 66(3), pp. 277–285, 2022

Critical Clearing Time and Angle for Power Systems Postfault Stability Assessment

Lounis Latiki[1*], Abdallah Medjdoub[1], Nabil Taib[2]

[1] Laboratoire de Génie Electrique de Bejaia (LGEB), Faculté de Technologie, Université de Bejaia, 06000 Bejaia, Algeria
[2] Laboratoire de Technologie Industrielle et de l'Information (LTII), Faculté de Technologie, Université de Bejaia, 06000 Bejaia, Algeria
* Corresponding author, e-mail: lounis.latiki@univ-bejaia.dz

Received: 16 January 2022, Accepted: 29 April 2022, Published online: 08 June 2022

Abstract

Transient stability analysis is a very important tool to deal with many behaviors of electrical power systems during and after being subjected to various disturbances. this paper propose a method for electrical power systems transient stability assessment using phase plane trajectories. A methodology for computing the critical stability conditions of generators is proposed. The critical conditions such as critical clearing time (CCT) and critical clearing angle (CCA) were obtained. The computation of CCA and CCT is curried out step by step using the characteristics of the faulted and postfault trajectories from given initial conditions until their intersection point. The angle and time values founded represent, by definition, the critical conditions of the system. The proposed algorithm can be used for complex models since it is based on solving systems of differential equations by iterative methods in the phase plane. The advantage provided by this method is it's accurate and small time consuming. To demonstrate the effectiveness of the proposed method, first, critical conditions calculation procedures are given, then the process used in judging power system stability is provided, finally, simulation results for various test cases of a single machine infinite bus (SMIB) system highlight the proposed methodology.

Keywords

transient stability, phase plane analysis, modified euler's mehod, critical clearing time, critical clearing angle

1 Introduction

Power system stability is the ability of an electric power system, at a given initial operating state, to restore a state of stable operating equilibrium after being subjected to some disturbances. The main kinds of these disturbances are a changing in loads, a changing in network configuration and a severe faults in the system. In other hand, we can define power system instability as a loss of synchronism when he is subjected to a particular disturbance. The main objective of the stability analysis in power system is to keep the whole system intact by ensuring the accuracy of transfer capability of transmission lines and identifying the potential disturbances that could lead to instabilities.

Stability analysis of power systems involves the computation of the nonlinear transient dynamic trajectory of the postfault system, which depends on the initial operating conditions, the nature and duration as well as magnitude of the perturbation.

The rotor angle deviation of the synchronous machine during transient period is used as an index to assess its ability to maintain or restore equilibrium between electromagnetic and mechanical torques by analyzing the electromechanical oscillations inherent in power systems. Several classes of methods are developed to obtain transient stability limits of power systems. Time-domain simulation (TDS) methods via numerical integration are largely used in transient stability study. Numerical methods, by solving the second order nonlinear differential swing equation, using time-domain numerical integration are the most accurate and very efficient given their ability to analyze very complex nonlinear mathematical models. This is, because they take into account all the phenomena present in the system. The main drawback of these approaches is that they are time consuming and require the whole system of equations for assessing stability of large power systems [1–4].

Alternatively, Lyapunov's direct methods (DM), have been proposed in many research papers [5–10]. The main application of these class of methods is to check whether the postfault trajectory will converge to an acceptable steady-state

Cite this article as: Latiki, L., Medjdoub, A., Taib, N. "Critical Clearing Time and Angle for Power Systems Postfault Stability Assessment", Periodica Polytechnica Electrical Engineering and Computer Science, 66(3), pp. 277–285, 2022. https://doi.org/10.3311/PPee.19858

as time proceeds. By using positive-definite Lyapunov functions, these methods, assess stability region of the post-fault equilibrium without resorting to numerical integration. Another advantage is that they can evaluate a large scale power systems stability via total energy present in the system using transient energy functions (TEF) [7–10]. However, these methods suffer from certain drawbacks which have posed challenges in several researches, such as the absence of an analytical procedure to find the appropriate TEF and the critical energy values, which exist only for a small and limited category of mathematical models. This insufficiency affect the accuracy of stability assessment.

New development ways are to combine direct method and time-domain method into an integrated power system stability program to take the merits of both methods [11–13]. This combination known as hybrid methods, is used for stability assessment by computing the actual trajectory using TDS then evaluating the TEF for decision making. These type of methods are faster than TDS in computation time and more accurate than DM in estimating stability margin, but they are relatively slow compared with DM.

Other methods like machine learning (ML) methods have been proposed for power system transient stability analysis. In [14], a power system stability is performed via artificial neural network algorithm, where the TDS and lots parameter settings are needed for training data acquisition. However, there is no way to escape from the excessive training time and complex parametrizations generated by such method. These methods are complex and time consuming [14–17].

In recent years, phase plane trajectory analysis (PPTA) methods have been proposed for power system transient stability analysis [18–21].

In this paper, a power systems transient stability assessment using phase plane trajectories is presented. This technique use both faulted and critical postfault trajectories to compute critical conditions such as CCT and CCA.

It is well known that the phase plane representation is a graphical method used to study the solutions of second order nonlinear differential equations. The principle of this method is to visualize the solutions of the equations in the phase plane, which correspond to system trajectories for different initial conditions. The obtained trajectories are called the phase portrait of the system and have important proprieties.

1.1 Mathematical basic concepts

Considering the autonomous nonlinear second order system expressed by Eq. (1):

$$\ddot{x} = f\left(\dot{x}, x\right). \tag{1}$$

Described in the state representation by Eq. (2):

$$\begin{cases} \dot{x}_1 = x_2 \\ \dot{x}_2 = f\left(x_1, x_2\right) \end{cases}, \tag{2}$$

where:

$$x_1 = x\,, \tag{3}$$

$$x_2 = \dot{x}_1\,, \tag{4}$$

are the state variables.

The solution of Eq. (2) is plotted in a graphic whose horizontal and vertical coordinates are x_1, x_2, respectively. A such graphic is called phase plane. This representation can be found with Eq. (5) derived from Eq. (2) by dividing the second over the first equations.

$$\frac{dx_2}{dx_1} = \frac{f_1\left(x_1, x_2\right)}{f_2\left(x_1, x_2\right)}, \tag{5}$$

where:

$$f_1\left(x_1, x_2\right) = f\left(x_1, x_2\right), \tag{6}$$

$$f_2\left(x_1, x_2\right) = x_2\,. \tag{7}$$

The system Eq. (2) can have more than one equilibrium point which are also singular points of Eq. (5), and which verify:

$$\dot{x}_1 = \dot{x}_2 = 0 \text{ or } f_1\left(x_1, x_2\right) = f_2\left(x_1, x_2\right) = 0\,.$$

For each equilibrium point, the behavior of the system Eq. (2) in the neighborhood of equilibrium points is determined by analyzing the eigenvalues λ_1, λ_2 and eigenvectors V_1, V_2 of the linearized system given by Eq. (8). For more details see [20].

$$J = \begin{bmatrix} \dfrac{\partial k_1\left(x_1, x_2\right)}{\partial x_1} & \dfrac{\partial k_1\left(x_1, x_2\right)}{\partial x_2} \\ \dfrac{\partial k_2\left(x_1, x_2\right)}{\partial x_1} & \dfrac{\partial k_2\left(x_1, x_2\right)}{\partial x_2} \end{bmatrix} \tag{8}$$

For the stable equilibrium point, the eigenvalues obtained are both complex with negative real part for the damped systems, and imaginary with zero real parts for the undamped systems. For the unstable point, the eigenvalues obtained λ_1, λ_2 are real with opposite signs [22].

Eigenvectors obtained from linearized system have very important characteristic which determine the direction and represents the slopes of trajectories in a local small neighborhood of equilibrium points, where those corresponding to positive eigenvalues are called unstable whereas those corresponding to negative eigenvalues are called stable ones which will be used further as initial conditions.

2 Main procedures of the proposed technique

This section aims to determine stability limits of an electric power system modelled by Eq. (2). These latters are obtained from solving Eq. (5) for two possible situations *a* and *b* that the system could be in, during fault and after fault respectively.

For situation *a*: $\frac{dx_2}{dx_1} = g(x_1, x_2)$. (9)

For situation *b*: $\frac{dx_1}{dx_2} = h(x_1, x_2)$, (10)

g and *h* are parameterized functions of the situations *a* and *b* respectively.

In power systems, the intersection of the solutions expressed by equations Eq. (9) and Eq. (10) in the phase plane, which are called further in the next sections faulted and postfault dynamics, gives us quantitative information that are sufficient for stability judgement. To obtain the intersection point (x_1, x_2) shown in Fig. 1, which gives us the critical conditions such as CCT and CCA that we detail in Section 4, we compute:

- The two trajectories $Cf(x_1)$, $Cp(x_1)$, curve fault and postfault respectively, from starting points $(x_{1,i}, x_{2,i})$ and $(x_{1,j}, x_{2,j})$ to the intersection point $(x_{1,c}, x_{2,c})$.

This procedure is illustrated in Fig. 1, where the succession of steps numerated from one to four describe the steps needed to compute $Cf(x_1)$, $Cp(x_1)$ from $(x_{1,i}, x_{2,i})$ and $(x_{1,j}, x_{2,j})$ until $(x_{1,c}, x_{2,c})$ point by point.

3 Power system modeling and analysis

3.1 Classical model

Consider a SMIB power system given in Fig. 2.

The mathematical model of such system is expressed with the second order differential equation given by Eq. (11):

$$M\ddot{\delta} + D\dot{\delta} = P_m - P_{\max} \operatorname{Sin}\delta \,. \quad (11)$$

Eq. (11) can be expressed by a set of first order differential equations given by Eq. (12), with state variables δ–ω, using Eq. (3) and Eq. (4) as follow:

$$\begin{cases} \dot{\delta} = \omega \\ M\dot{\omega} = P_m - P_{\max} \operatorname{Sin}(\delta) - D\omega \end{cases}, \quad (12)$$

where:

δ: power angle in radians

ω: relative velocity in (radians per seconds)

P_m: mechanical power input in (pu)

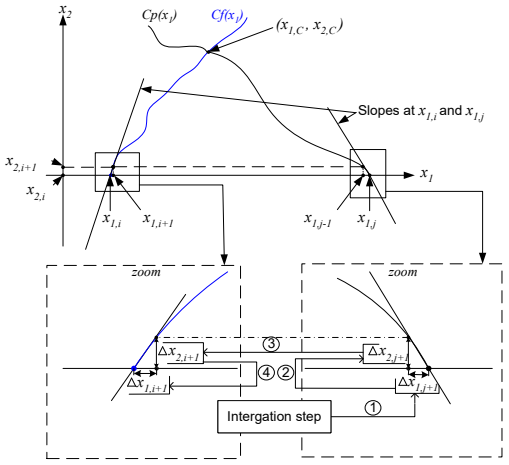

Fig. 1 Main procedures of the proposed method

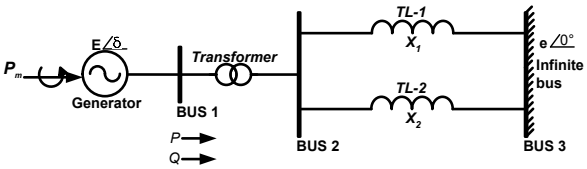

Fig. 2 Single machine infinite bus system

$P_{\max}$: maximum electrical power output of a synchronous generator in (pu)

D: damping coefficient

M: inertia constant of the generator.

The behavior of power system during transient period is described in three stages as follows:

Stage 01:

Initially ($t < 0$), the power system is operating at its stable steady state equilibrium conditions and it is expressed with a set of differential equations given by Eq. (13):

$$\begin{cases} \dot{\delta} = \omega \\ M\dot{\omega} = P_m - P_{pre} \operatorname{Sin}(\delta) - D\omega \end{cases}, \quad (13)$$

where:

P_{pre}: maximum power output of the generator before the fault in (pu).

With the stable and unstable equilibrium points

$$((\delta^o = \operatorname{Sin}^{-1}\frac{P_m}{P_{pre}}, \omega^o = 0),\ (\delta^{ou} = \pi - \operatorname{Sin}^{-1}\frac{P_m}{P_{pre}}, \omega^{ou} = 0))$$

respectively.

Stage 02:

Assume that at $t = 0$, a three phase short circuit occurs at any point in the given system. In this situation, the system is governed by the fault dynamics given by Eq. (14):

$$\begin{cases}\dot{\delta} = \omega \\ M\dot{\omega} = P_m - P_f \operatorname{Sin}(\delta) - D\omega \end{cases}, \tag{14}$$

where:

P_f: maximum power output of the generator during the fault in (pu).

Note that the initial conditions $(\delta^o = \operatorname{Sin}^{-1}\frac{P_m}{P_{pre}}, \omega^o = 0)$ of this faulted period are the stable operating conditions of the pre-fault period.

Stage 03:

When the fault is cleared at $t = t_{cl}$ by action of protective system operations, the system is governed by the postfault dynamics given by Eq. (15):

$$\begin{cases}\dot{\delta} = \omega \\ M\dot{\omega} = P_m - P_a \operatorname{Sin}(\delta) - D\omega \end{cases}, \tag{15}$$

where:

P_a: maximum power output of the generator after the fault in (pu).

With stable and unstable equilibrium points

$(\delta^s = \operatorname{Sin}^{-1}\frac{P_m}{P_a}, \omega^s = 0)$, $(\delta^u = \pi - \operatorname{Sin}^{-1}\frac{P_m}{P_a}, \omega^u = 0)$

respectively.

The initial conditions $(\delta = \delta_{cl}, \omega = \omega_{cl})$ of this postfault period are the angle and velocity of the generator at the instant of clearing of the fault.

3.2 Postfault system stability analysis

In order to check either the postfault system is stable or not, let's define:

- δ_{cr} and ω_{cr} as the critical angle and critical velocity, given by the horizontal and vertical coordinates respectively, obtained from the intersection of the critical postfault and fault trajectories represented in the phase plane portrait as shown in Fig. 3.
- The critical trajectory of the postfault system governed by the postfault dynamics is the path linking the two points $(\delta_{cr}, \omega_{cr})$, (δ_u, ω_u).

According to the representation above, the postfault system is:

Stable if: $\delta_{cr} > \delta_{cl}$, case where $\delta_{cl} = \delta_{cl1}$.

Unstable if: $\delta_{cr} < \delta_{cl}$, case where $\delta_{cl} = \delta_{cl3}$.

Critical if: $\delta_{cr} = \delta_{cl}$.

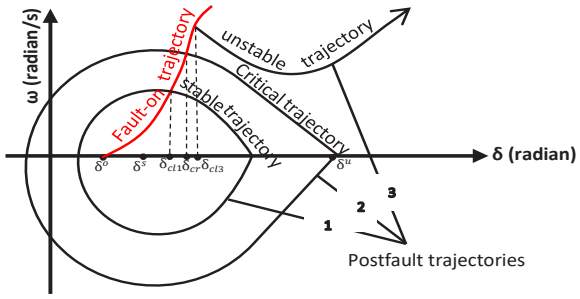

Fig. 3 Phase plane trajectories representation

4 Algorithm of the method

The proposed technique uses an algorithm based on Modified Euler's Method which compute critical conditions simultaneously, (CCT) and (CCA), using the phase plane plot of during fault and postfault conditions.

4.1 Phase plane plot of during fault conditions

The faulted period is characterized by:

- The maximum transfer power of the generator (P_f) obtained from the change of the network configuration during the fault conditions.
- Initial conditions $(\delta°, \omega°)$ which are steady state stable operating conditions of the pre-fault period.

The fault trajectory is obtained step by step using Eq. (16) built from Eq. (14) in the same manner as Eq. (5):

$$\frac{d\delta}{d\omega} = \frac{M\omega}{P_m - P_f \operatorname{Sin}(\delta) - D\omega} \tag{16}$$

For a small increment $\Delta\omega_f^{i+1}$ defined by Eq. (17), $\Delta\delta_f^{i+1}$ is obtained by applying Modified Euler's method as follow:

$$\Delta\omega_f^{i+1} = \omega_f^{i+1} - \omega_f^i \tag{17}$$

$$\Delta\delta_f^{i+1} = \frac{\Delta\omega_f^{i+1}}{2}\left[\left(\frac{d\delta}{d\omega}\right)\Big|_{\substack{\delta=\delta_f^i \\ \omega=\omega_f^i}} + \left(\frac{d\delta}{d\omega}\right)\Big|_{\substack{\delta=\delta_f^{i+1} \\ \omega=\omega_f^{i+1}}}\right] \tag{18}$$

$$\Delta\delta_f^{i+1} = \delta_f^{i+1} - \delta_f^i \tag{19}$$

4.2 Phase plane plot of the postfault conditions

When the fault is cleared, a change in system configuration occurs and a new maximum transfer power P_a is obtained. Then the postfault trajectory is computed step by step using Eq. (20) built from Eq. (15) in the same manner as Eq. (5).

$$\frac{d\omega}{d\delta} = \frac{P_m - P_a \operatorname{Sin}(\delta) - D\omega}{M\omega} \tag{20}$$

For a small increment $\Delta\delta_a^{i-1}$ defined by Eq. (21), $\Delta\omega_a^{i-1}$ is obtained by applying Modified Euler's method as follow:

$$\Delta\delta_a^{i-1} = \delta_a^{i-1} - \delta_a^i \tag{21}$$

$$\Delta\omega_a^{i-1} = \frac{\Delta\delta_a^{i-1}}{2}\left[\left(\frac{d\omega}{d\delta}\right)\Big|_{\substack{\delta=\delta_a^i \\ \omega=\omega_a^i}} + \left(\frac{d\omega}{d\delta}\right)\Big|_{\substack{\delta=\delta_a^{i-1} \\ \omega=\omega_a^{i-1}}}\right] \tag{22}$$

$$\Delta\omega_a^{i-1} = \omega_a^{i-1} - \omega_a^i \tag{23}$$

The critical trajectory of the postfault system is plotted from $\left(\delta_a^i = \delta^u, \omega_a^i = \omega^u\right)$ to $(\delta_{cr}, \omega_{cr})$ with the set of initial conditions (δ^u, ω^u) and $\left(\frac{d\omega}{d\delta}\right)\Big|_{\substack{\delta=\delta^u \\ \omega=\omega^u}}$,
where:
$\left(\frac{d\omega}{d\delta}\right)\Big|_{\substack{\delta=\delta^u \\ \omega=\omega^u}}$ represent the slope of the stable eigenvector obtained from the linearization of the postfault system around the saddle equilibrium point (δ^u, ω^u).

4.3 CCT calculation from trajectories

During the fault time period, CCT is obtained step by step from the plot of the faulted trajectory using Eq. (24):

$$dt = \frac{d\delta}{\omega} \tag{24}$$

for a small increment $\Delta\delta_f^{i+1}$ defined by Eq. (19), an interval of time Δt_f^{i+1} is obtained by Eq. (25):

$$\Delta t_f^{i+1} = \frac{\Delta\delta_f^{i+1}}{\left(\omega_f^{i+1} + \omega_f^i\right)/2}, \tag{25}$$

where $\left(\omega_f^{i+1} + \omega_f^i\right)/2$ is the average velocity in the interval $\Delta\delta_f^{i+1}$, then the time is given by Eq. (26):

$$t_f^{i+1} = t_f^i + \Delta t_f^{i+1}. \tag{26}$$

The procedures for computing critical conditions are resumed as follows:

First, negatif $\Delta\delta_a^{i-1}$ is fixed and then $\Delta\omega_a^{i-1}$ is obtained by Eq. (22). The increment ω_a^{i-1} is obtained from Eq. (23).

Second, the obtained increment $\Delta\omega_a^{i-1}$ is used as an increment $\Delta\omega_f^{i+1}$ in Eq. (18) then $\Delta\delta_f^{i+1}$ is obtained. The increment $\Delta\delta_f^{i+1}$ is obtained from Eq. (19).

Finally, the time is obtained directly by Eq. (25) and Eq. (26).

The process is stopped at iteration n when $(\delta_a^{i-n} - \delta_f^{i+n})$ achieve its minimum positive value, then the critical conditions are directly obtained and compared to the real clearing time t_{cl} for stability judgment. In Fig. 4, a flow chart of the proposed algorithm shows how the stability decision is taken.

5 Simulation results and analysis

Fig. 5 shows SMIB power system model taken from [23] used to test the proposed algorithm. It consists of four 555 MVA, 24 kV, 60 Hz units supplying power to an infinite bus through two transmission lines.

The network reactances shown in Fig. 5 are expressed in per unit on 2220 MVA, 24 kV base with resistances neglected.

The generators are modeled as SMIB supplying power to an infinite bus with following parameters expressed in per units on 2220 MVA, 24 kV base. The SMIB system parameters are listed in Table 1.

The initial operating conditions of the system are also given in per unit on 2220 MVA, 24 kV base by:

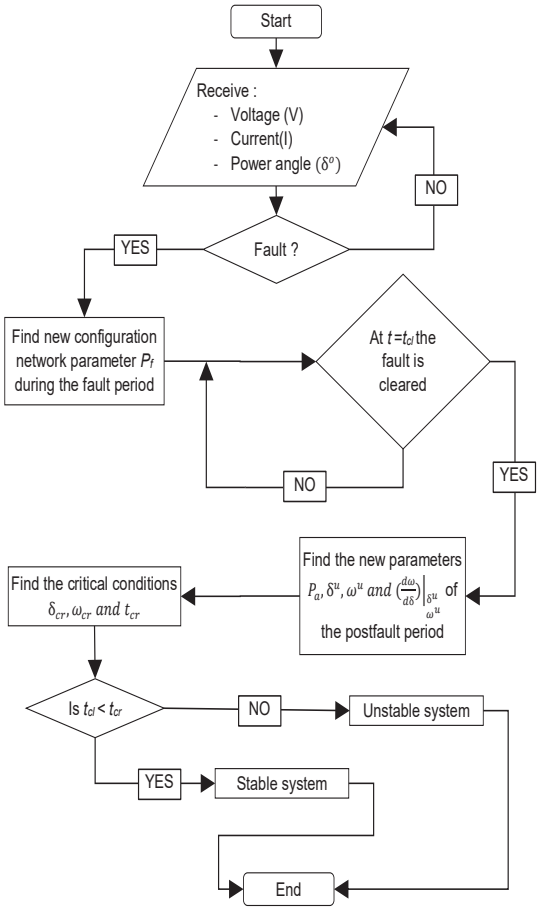

Fig. 4 Flow chart of the proposed algorithm

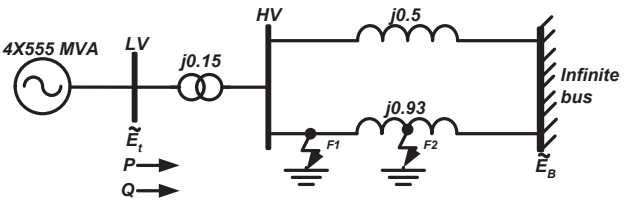

Fig. 5 SMIB test system

Table 1 SMIB data

Equipment	Parameter	Value
Generators	S (MVA)	4X555
	Rating voltage (kV)	24
	Direct axis transient reactance X_d' (pu)	0.3
	Inertia constant H (MW s/MVA)	3.5
	Frequency (Hz)	60
Transformers	Reactances (pu)	0.15
Transmission lines	TL-1 Reactance (pu)	0.5
	TL-2 Reactance (pu)	0.93

P = 0.9 pu, Q = 0.436 pu (overexcited), terminal bus and infinite bus voltages are $\tilde{E}_t$ = 1.0, $\tilde{E}_B$ = 0.90081 with angles 28.23°, 0° respectively.

The algorithm is tested for two faults locations F1 and F2, with and without damping coefficient D and the critical conditions are chosen as the limit of stability conditions, beyond this limit the system will be unstable.

The obtained results are compared to those obtained from conventional fourth order Runge-Kutta simulation method.

In Tables 2–7, the obtained values of CCTs and CCAs are listed for different fault locations, damping coefficient values D and number of iterations n. The CCT and CCA obtained by the Runge-Kutta method is also given for comparison purposes, and for each case study, the phase plane trajectories obtained by both the proposed technique (PM) and Runge-Kutta method (RK) used to find CCA and CCT are given in Figs. 6–11.

Case 01

Fault location at F1

- for period during fault: $\delta° = 0.7291$ rad, $\omega° = 0$ rad per second with maximum power transfer $P_f = 0$ pu.
- For the postfault period: $\delta^u = \pi - \delta^s = 2.1864$ rad, $\omega^u = 0$, $P_a = 1.1024$ pu and $\left(\frac{d\omega}{d\delta}\right)\Big|_{\substack{\delta=\delta^u \\ \omega=\omega^u}} = -5.8604$, where $\left(\frac{d\omega}{d\delta}\right)\Big|_{\substack{\delta=\delta^u \\ \omega=\omega^u}}$ is the stable eigenvector of the linearized system around the equilibrium (δ^u, ω^u).
- The Step of integration is obtained by dividing the interval [$\delta°$, δ^u] to n + 1 points and is given by $\Delta\delta_a = -(\delta^u - \delta°)/n$.

Case 02

Fault location at F2

For period during fault: $\delta° = 0.7291$ rad, $\omega° = 0$ rad per second with maximum power transfer $P_f = 0.7307$ pu.

For the postfault period: $\delta^u = \pi - \delta^s = 2.1864$ rad, $\omega^u = 0$, $P_a = 1.1024$ pu and $\left(\frac{d\omega}{d\delta}\right)\Big|_{\substack{\delta=\delta^u \\ \omega=\omega^u}} = -5.8604$.

Table 2 CCT and CCA of a SMIB test in the case of F1 and D = 0

Critical conditions	Proposed method				RK- 4th order	Distance (PM vs RK)	
	n_1 = 100	n_2 = 1000	n_3 = 9000	$\Delta t = 10^{-7}$	n_1 vs Δt	n_2 vs Δt	n_3 vs Δt
δ_{cr} (radian)	0.9119	0.9118	0.9118	0.9117	0.0002	0.0001	0.0001
t_{cr} (second)	0.0851	0.0867	0.0868	0.0868	0.0017	0.0001	0.0000

Table 3 CCT and CCA of a SMIB test in the case of F1and D = 0.01

Critical conditions	Proposed method				RK- 4th order	Distance (PM vs RK)	
	n_1 = 100	n_2 = 1000	n_3 = 9000	$\Delta t = 10^{-7}$	n_1 vs Δt	n_2 vs Δt	n_3 vs Δt
δ_{cr} (radian)	0.9595	0.9596	0.9597	0.9584	0.0011	0.0012	0.0013
t_{cr} (second)	0.0966	0.0982	0.0984	0.0979	0.0013	0.0003	0.0005

Table 4 CCT and CCA of a SMIB test in the case of F1 and D = 0.02

Critical conditions	Proposed method				RK- 4th order	Distance (PM vs RK)	
	n_1 = 100	n_2 = 1000	n_3 = 9000	$\Delta t = 10^{-7}$	n_1 vs Δt	n_2 vs Δt	n_3 vs Δt
δ_{cr} (radian)	1.0090	1.0107	1.0108	1.0075	0.0015	0.0032	0.0033
t_{cr} (second)	0.1078	0.1097	0.1099	0.1089	0.0011	0.0008	0.0010

Table 5 CCT and CCA of a SMIB test in the case of F2 and D = 0

Critical conditions	Proposed method				RK- 4th order	Distance (PM vs RK)	
	n_1 = 100	n_2 = 1000	n_3 = 9000	$\Delta t = 10^{-7}$	n_1 vs Δt	n_2 vs Δt	n_3 vs Δt
δ_{cr} (radian)	1.2052	1.2128	1.2128	1.2126	0.0074	0.0002	0.0002
t_{cr} (second)	0.2142	0.2196	0.2199	0.2199	0.0057	0.0003	0.0000

Table 6 CCT and CCA of a SMIB test in the case of F2 and D = 0.01

Critical conditions	Proposed method				RK- 4th order	Distance (PM vs RK)	
	n_1 = 100	n_2 = 1000	n_3 = 9000	$\Delta t = 10^{-7}$	n_1 vs Δt	n_2 vs Δt	n_3 vs Δt
δ_{cr} (radian)	1.3031	1.3155	1.3168	1.3089	0.0058	0.0066	0.0079
t_{cr} (second)	0.2442	0.2507	0.2514	0.2484	0.0042	0.0023	0.0030

Table 7 CCT and CCA of a SMIB test in the case of F2 and D = 0.02

Critical conditions	Proposed method				RK- 4th order	Distance (PM vs RK)	
	n_1 = 100	n_2 = 1000	n_3 = 9000	$\Delta t = 10^{-7}$	n_1 vs Δt	n_2 vs Δt	n_3 vs Δt
δ_{cr} (radian)	1.3944	1.4188	1.4192	1.4025	0.0081	0.0163	0.0167
t_{cr}(second)	0.2742	0.2838	0.2842	0.2774	0.0032	0.0064	0.0072

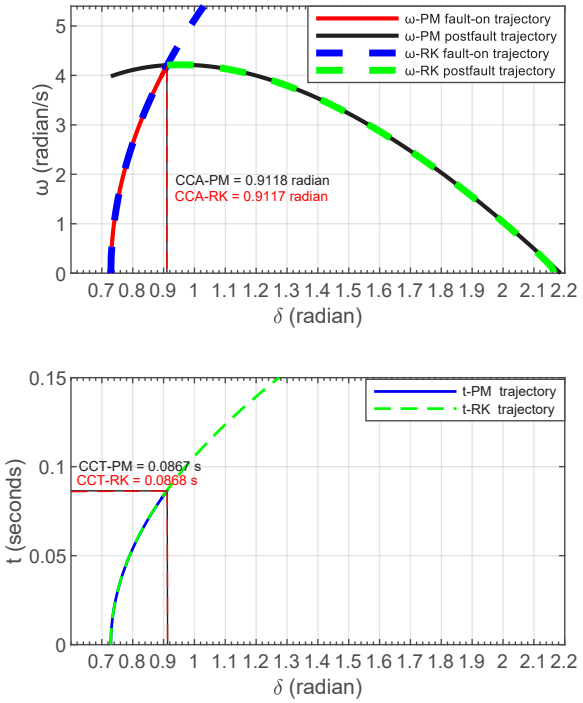

Fig. 6 Phase plane trajectories used to find CCA and CCT in the case of F1 and $D = 0$

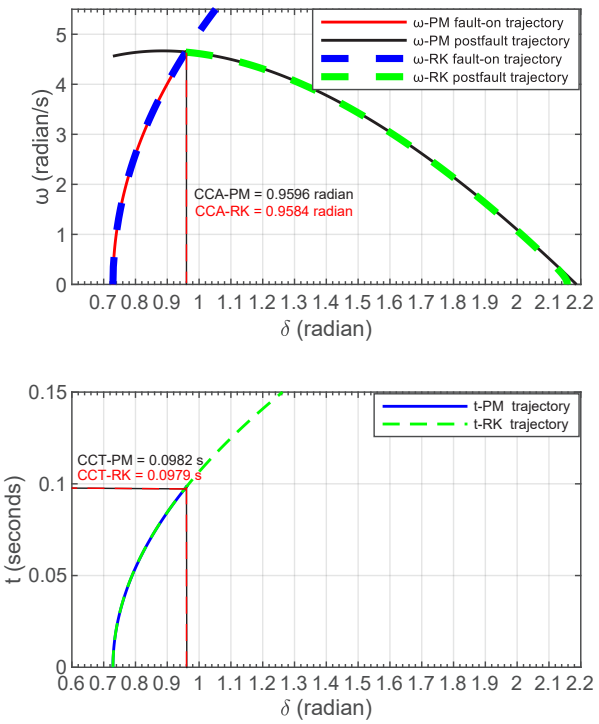

Fig. 7 Phase plane trajectories used to find CCA and CCT in the case of F1 and $D = 0.01$

Simulation results obtained in Tables 2–7 show that the critical conditions obtained by the proposed algorithm are not conservative and they are very closest to those obtained by the conventional RK 4th order numerical simulation method with very small integration step.

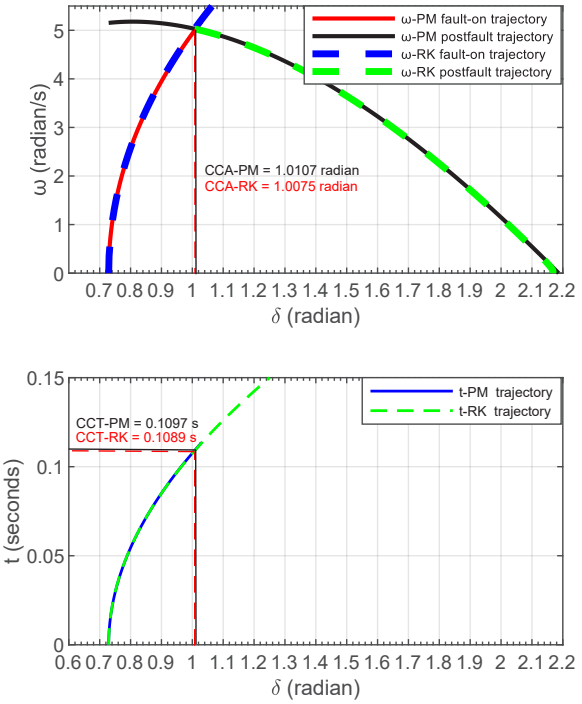

Fig. 8 Phase plane trajectories used to find CCA and CCT in the case of F1 and $D = 0.02$

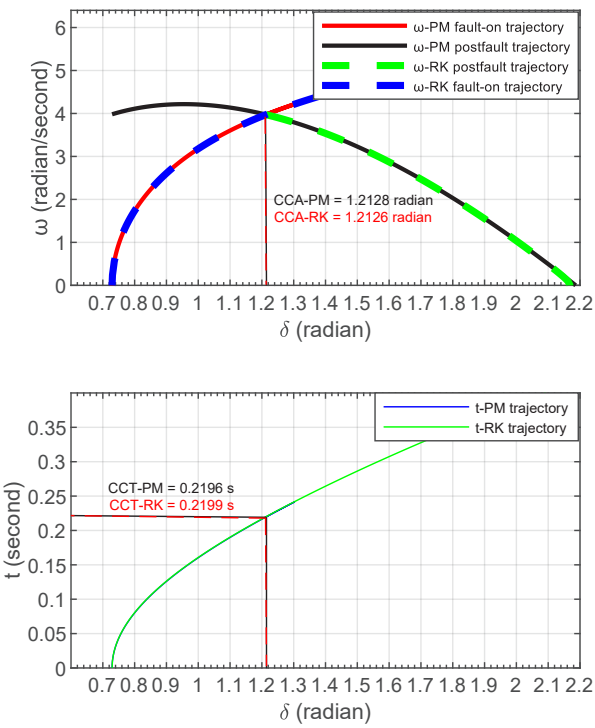

Fig. 9 Phase plane trajectories used to find CCA and CCT in the case of F2 and $D = 0$

It is well known that, numerical methods perform high accuracy when the integration step is relatively small. For this purpose and to show the effectiveness of the proposed method, the results are discussed for RK 4th integration step Δt of 10^{-7} and for the proposed method iterations number n of 9000.

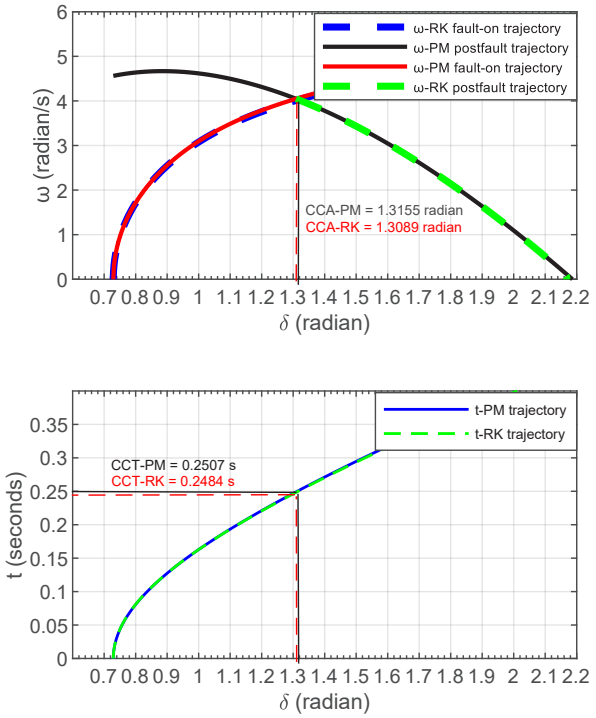

Fig. 10 Phase plane trajectories used to find CCA and CCT in the case of F2 and $D = 0.01$

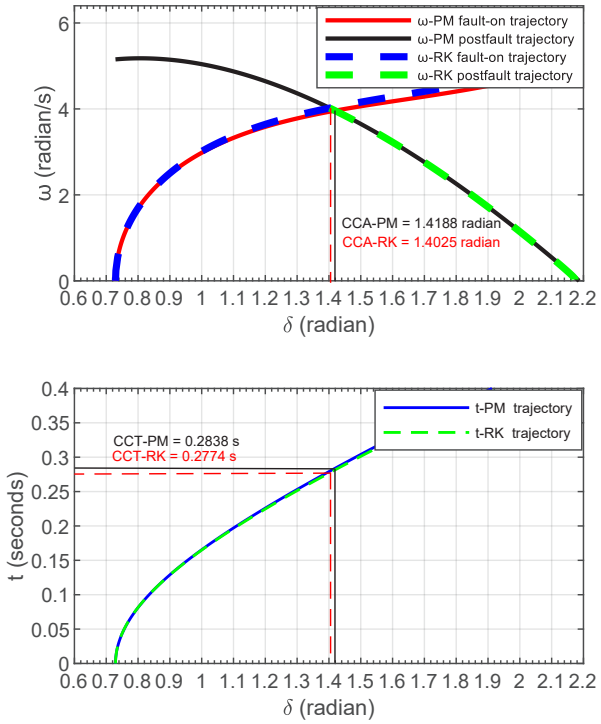

Fig. 11 Phase plane trajectories used to find CCA and CCT in the case of F2 and $D = 0.02$

In Tables 2 and 5, where the coefficient D is set to zero; and for the two different fault locations F1 and F2, the CCTs obtained by both methods are 0.0868 seconds and 0.2199 seconds, respectively. For the same situation, the CCA obtained by the two methods are slightly different and distant from each other around 10^{-4} radians and the data presented in Tables 3–4 and Tables 6–7 shows that as the damping coefficient increases, the difference in CCT and CCA values provided by both methods increases but it remains weak.

Figs. 6–11 show the time t-PM and the relative velocity ω-PM superposed trajectories obtained by proposed method compared to t-RK and ω-RK obtained by the conventional RK 4th order simulation method, where the plots show critical conditions, CCA and CCT obtained by both proposed method CCA-PM and CCT-PM, and Runge-Kutta method CCA-RK and CCT-RK respectively. It is clearly shown that these critical conditions are very closest to each other.

6 Conclusion

Transient stability analysis is a very useful tool to avoid the instabilities in power systems networks after being subjected to disturbances. In this paper, a power system transient stability assessment using phase plane representation is proposed. The approach uses phase plane faulted and postfault trajectories to obtain the critical conditions CCA and CCT simultaneously. The proposed method doesn't need additional time after clearing time to confirm if the system remains stable or not after being subjected to perturbation. This is because the two trajectories are also computed simultaneously using characteristics of the stable and unstable equilibriums of the system studied. In other words, the clearing time of the real system is compared to the CCT computed by the method then decision is taken.

The critical conditions obtained are very closest to those obtained by RK 4th order conventional simulation method with and without integrating damping coefficient. Also, obtained results, show that the damping coefficient has an important effect on transient stability improvement which can't be shown by direct methods, moreover, the proposed methodology is faster than time domain simulation methods in computational time and most accurate than direct methods which perform conservative results.

References

[1] Sauer, P. W., Pai, M. A., Chow, J. H. "Power System Dynamics and Stability", Wiley, West Sussex, UK, 2017. ISBN 978-1-119-35577-9

[2] Dong, Y., Pota, H. R. "Fast transient stability assessment using large step-size numerical integration", IEE Proceedings C (Generation, Transmission and Distribution), 138(4), pp. 377–383, 1991. https://doi.org/10.1049/ip-c.1991.0047

[3] Padhi, S., Mishra, B. P. "Numerical Method Based Single Machine Analysis for Transient Stability", International Journal of Emerging Technology and Advanced Engineering, 4(2), pp. 330–335, 2014.

[4] Su, F., Zhang, B., Yang, S., Wang, H. "A Novel Termination Algorithm Of Time-Domain Simulation For Power System Transient Stability Analysis Based On Phase-Plane Trajectory Geometrical Characteristic", In: IEEE 5th International Conference on Electric Utility Deregulation and Restructuring and Power Technologies, Changsha, China, 2015, pp. 1422–1426. https://doi.org/10.1109/DRPT.2015.7432455

[5] Owusu-Mireku, R., Chiang, H.-D. "A Direct Method for the Transient Stability Analysis of Transmission Switching Events", In: 2018 IEEE Power and Energy Society General Meeting (PESGM), Portland, OR, USA, 2018, pp. 1–5. https://doi.org/10.1109/PESGM.2018.8586242

[6] Shuai, Z., Shen, C., Liu, X., Li, Z., Shen, Z. J. "Transient Angle Stability of Virtual Synchronous Generators Using Lyapunov's Direct Method", IEEE Transactions on Smart Grid, 10(4), pp. 4648–4661, 2019. https://doi.org/10.1109/TSG.2018.2866122

[7] Amte, A. Y., Kate, P. S. "Automatic generation of Lyapunov function using Genetic programming approach", In: 2015 IEEE International Conference on Energy Systems and Applications, Pune, India, 2015, pp. 771–775. https://doi.org/10.1109/ICESA.2015.7503454

[8] Rimorov, D., Wang, X., Kamwa, I., Joós, G. "An Approach to Constructing Analytical Energy Function for Synchronous Generator Models with Subtransient Dynamics", IEEE Transactions on Power Systems, 33(6), pp. 5958–5967, 2018. https://doi.org/10.1109/TPWRS.2018.2829887

[9] Han, D., El-Guindy, A., Althoff, M. "Power Systems Transient Stability Analysis via Optimal Rational Lyapunov Functions", In: 2016 IEEE Power and Energy Society General Meeting, Boston, MA, USA, 2016, pp. 1–5. https://doi.org/10.1109/PESGM.2016.7741322

[10] Wu, D., Ma, F., Jiang, J. N. "A study on relationship between power network structure and total transient energy", Electric Power Systems Research, 143, pp. 760–770, 2017. https://doi.org/10.1016/j.epsr.2016.10.019

[11] Veerashekar, K., Schuehlein, P., Luther, M. "Quantitative transient stability assessment in microgrids combining both time-domain simulations and energy function analysis", International Journal of Electrical Power and Energy Systems, 115, 105506, 2020. https://doi.org/10.1016/j.ijepes.2019.105506

[12] Kyesswa, M., Çakmak, H. K., Gröll, L., Kûhnapfel, U., Hagenmeyer, V. "A Hybrid Analysis Approach for Transient Stability Assessment in Power Systems", In: 2019 IEEE Milan PowerTech, Milan, Italy, 2019, pp. 1–6. https://doi.org/10.1109/PTC.2019.8810745

[13] Bonvini, B., Massucco, S., Ivlorini, A., Siewierski, T. "A Comparative Analysis of Power System Transient Stability Assessment by Direct and Hybrid Methods", In: Proceedings of 8th Mediterranean Electrotechnical Conference on Industrial Applications in Power Systems, Computer Science and Telecommunications (MELECON 96), Bari, Italy, 1996, pp. 1575–1579. https://doi.org/10.1109/MELCON.1996.551253

[14] Shahzad, U. "Probabilistic Transient Stability Assessment of Power Systems Using Artificial Neural Networks", Journal of Electrical Engineering, Electronics, Control and Computer Science, 8(1), pp. 35–42, 2022.

[15] Guo, T., Milanović, J. V. "Probabilistic Framework for Assessing the Accuracy of Data Mining Tool for Online Prediction of Transient Stability", IEEE Transactions on Power Systems, 29(1), pp. 377–385, 2014. https://doi.org/10.1109/TPWRS.2013.2281118

[16] Li, Y., Yang, Z. "Application of EOS-ELM With Binary Jaya-Based Feature Selection to Real-Time Transient Stability Assessment Using PMU Data", IEEE Access, 5, pp. 23092–23101, 2017. https://doi.org/10.1109/ACCESS.2017.2765626

[17] Huang, D., Yang, X., Chen, S., Meng, T. "Wide-area measurement system-based model-free approach of Postfault rotor angle trajectory prediction for on-line transient instability detection", IET Generation, Transmission and Distribution, 12(10), pp. 2425–2435, 2018. https://doi.org/10.1049/iet-gtd.2017.1523

[18] Su, F., Zhang, B., Yang, S., Wang, H. "Power System First-swing Transient Stability Detection Based on Trajectory Performance Of Phase-plane", In: 2016 IEEE PES Asia-Pacific Power and Energy Engineering Conference (APPEEC), Xi'an, China, 2016, pp. 2448–2451. https://doi.org/10.1109/APPEEC.2016.7779926

[19] Priyadi, A., Yorino, N., Eghbal, M., Zoka, Y., Sasaki, Y., Yasuda, H., Kakui, H. "Transient Stability Assessment as Boundary Value Problem", In: 2008 IEEE Canada Electric Power Conference, Vancouver, BC, Canada, 2008, pp. 1–6. https://doi.org/10.1109/EPC.2008.4763304

[20] Shrestha, B., Gokaraju, R., Sachdev, M. "Out-of-Step Protection Using State-Plane Trajectories Analysis", IEEE Transactions on Power Delivery, 28(2), pp. 1083–1093, 2013. https://doi.org/10.1109/TPWRD.2013.2245684

[21] Sajadi, A., Preece, R., Milanović, J. "Identification of transient stability boundaries for power systems with multidimensional uncertainties using index-specific parametric space", In: International Journal of Electrical Power and Energy Systems, 123, 106152, 2020. https://doi.org/10.1016/j.ijepes.2020.106152

[22] Marquez, H. J. "Nonlinear Control Systems", Wiley, 2003. ISBN 978-0-471-42799-5

[23] Kundur, P. "Power System Stability and Control", McGraw-Hill, 1994. ISBN 0-07-035958-X